CONF-810415--1

LA-UR-81-100

MASTER

TITLE: NODAL METHODS FOR DISCRETE-ORDINATES TRANSPORT PROBLEMS IN (X,Y) GEOMETRY

AUTHOR(S): Wallace F. Walters and R. Douglas O'Dell

SUBMITTED TO: ANS/ENS Joint Topical Meeting, Mathematical Methods in Nuclear Engineering, April 26-29, 1981, Munich, FRG

University of California

LOS ALAMOS SCIENTIFIC LABORATORY
Post Office Box 1663 Los Alamos, New Mexico 87545
An Affirmative Action/Equal Opportunity Employer

Form No. 836 R3
St. No. 2629
12/78

UNITED STATES
DEPARTMENT OF ENERGY
CONTRACT W-7405-ENG. 36

NODAL METHODS FOR DISCRETE-ORDINATES TRANSPORT PROBLEMS IN (X,Y) GEOMETRY

Wallace F. Walters and R. Douglas O'Dell
Theoretical Division
University of California
Los Alamos National Laboratory
Los Alamos, New Mexico 87545 USA

A nodal method has been developed for improved spatial differencing of the discrete-ordinates form of the x,y geometry transport equation. In applying this method, spatial flux expansions are assumed along the edges of each solution node (mesh cell) and flux and source expansions are assumed in the interior of the node. Nodal method schemes are thus identified by the expansions used for node edges and node interior. Nodal schemes assuming constant-constant, constant-linear, and four forms of linear-linear expansion have been developed, programmed, and used in the analysis of eigenvalue (k_{eff}) and shielding problems. Nodal results are compared with those obtained using the diamond-difference scheme.

Based on results of eigenvalue test problems examined by the authors, it appears that the linear-linear nodal method schemes are more cost effective than the diamond difference scheme for eigenvalue (k_{eff}) problems. These nodal schemes, although more computationally costly than the diamond scheme per mesh cell yield results of comparable accuracy to those from diamond with far fewer mesh cells. A net savings in both computer time and storage is obtained using the nodal schemes when compared with the diamond scheme for the same accuracy of results.

For shielding problems both the constant-linear and linear-linear nodal schemes are superior to the diamond scheme in the sense of reduced computer time and storage for the same accurary in results.

NODAL METHODS FOR DISCRETE-ORDINATES TRANSPORT PROBLEMS IN (X,Y) GEOMETRY

I. INTRODUCTION

In this work several nodal schemes applicable to the (x,y) geometry discrete-ordinates transport equation are developed. Contrary to many of the diffusion theory nodal methods which tend to be tailored to specific classes of problems[1], the transport nodal schemes we describe are used to generate spatial-differencing schemes for use in production computer codes.

In Reference 2 a hybrid type of nodal scheme is described. In this scheme a double P_1 approximation is used for angular distribution of interface currents. This approximation is not used in our method. The schemes we describe in this paper yield true discrete-ordinates results.

In a recent paper[3] a nodal transport scheme called the discrete nodal transport method (DNTM) was described and used to solve a one-group inhomogeneous source problem. DNTM assumes a quadratic flux expansion within the node and a constant flux representation on the node boundaries. The computer storage required with any node interior flux expansion (source expansion) of quadratic or higher order is likely to be prohibitive for a production code designed to solve a broad class of problems. Hence, we examine nodal schemes with node interior expansions up to and including linear and node boundary representations up to and including linear.

II. DEVELOPMENT OF THE NODAL EQUATIONS

Transport nodal methods can be characterized by the separate angular flux expansions assumed on the edges of a node (cell) and over the interior of the node. For example, a "constant-linear" method will, hereafter, refer to one in which independent constant edge angular flux "expansions" are assumed together with a linear flux expansion over the node interior.

Consider the i,j node to be the rectangle defined by $x_L \leq x \leq x_R$, $y_B \leq y \leq y_T$ and with $\Delta x = x_R - x_L$, $\Delta y = y_T - y_B$, $x_i = (x_L + x_R)/2$ and $y_j = (y_T + y_B)/2$. The discrete-ordinates equation for direction m and energy group g is

$$\mu_m \partial\Psi_{m,g}(x,y)/\partial x + \eta_m \partial\Psi_{m,g}(x,y)/\partial y + \sigma_g \Psi_{m,g}(x,y) = S_{m,g}(x,y) \quad . \tag{1}$$

Hereafter the subscripts m and g will be dropped.

We assume that the source within the node is (at most) linear, i.e.,

$$S(x,y) = S_{av} + S_x * 2(x - x_i)/\Delta x + S_y * 2(y - y_i)/\Delta y \qquad (2)$$

and that the source for a given iteration is determined using fluxes from the previous iteration. It is further assumed, for this analysis, that $\mu > 0$, $\eta > 0$ so that the fluxes on the node edges at x_L and y_B are known.

We represent the angular flux along the top edge of the node by, at most, a linear expansion:

$$\Psi(x,y_T) = \psi_T + \theta_T * 2(x - x_i)/\Delta x \quad \begin{cases} x_L < x < x_R \\ y = y_T \end{cases} \qquad (3)$$

with similar expansions for the other node edges.

Nodal equations are generated by performing transverse integrations of (1) over the node in the x- and y-directions. If we integrate (1) over $[x_L,x_R]$ there results an ordinary differential equation for $\Psi^o(y) \equiv$

$$\frac{1}{\Delta x}\int_{x_L}^{x_r} \Psi(x,y)\, dx :$$

$$\eta\, d\Psi^o(y)/dy + \sigma\Psi^o(y) = S_{av} + S_y * 2(y - y_j)/\Delta y - (\mu/\Delta x)\left[\Psi(x_R,y) - \Psi(x_L,y)\right] . \qquad (4)$$

We can also multiply (1) through by $(6/\Delta x^2)(x - x_i)$ and x-integrate over the node to get an equation for the y-dependent, first flux moment $\Psi^1(y) \equiv$

$$6/\Delta x^2 * \int_{x_L}^{x_R} (x - x_i)\, \Psi(x,y)\, dx :$$

$$\eta\, d\Psi^1(y)/dy + \sigma\Psi^1(y) = S_x + (6\mu/\Delta x)*\left\{ \Psi^o(y) - 0.5\left[\Psi(x_R,y) + \Psi(x_L,y)\right]\right\} . \qquad (5)$$

Similar expressions for $\Psi^o(x)$ and $\Psi^1(x)$ can be obtained by integrating in the y-direction.

Exact solutions to (4) and (5) are obtained and evaluated at $y = y_T$. These are:

$$\Psi^o(y_T) = \psi_T = \psi_B \exp(-\varepsilon_y) + (1/\eta)\int_{y_B}^{y_T} \exp\left[-\sigma\,(y_T - y)/\eta\right] * \left\{ S_{av} + (2/\Delta y)(y - y_j) * S_y - (\mu/\Delta x)\left[\Psi(x_R,y) - \Psi(x_L,y)\right]\right\} \tag{6}$$

and,

$$\Psi^1(y_T) = \theta_T = \theta_B \exp(-\varepsilon_y) + (1/\eta)\int_{y_B}^{y_T} \exp\left[-\sigma(y_T - y)/\eta\right] * \left\{ S_x + (6\mu/\Delta x)\left[\Psi^o(y) - 0.5\left[\Psi(x_R,y) + \Psi(x_L,y)\right]\right]\right\} \tag{7}$$

Similar exact expressions for $\Psi^o(x_R)$ and $\Psi^1(x_R)$ can also be generated. In these we define $\varepsilon_y \equiv \sigma\Delta y/\eta$, $\varepsilon_x \equiv \sigma\Delta x/\mu$.

III. SPECFIC NODAL SCHEMES

CC Scheme

The constant-constant (CC) scheme is our lowest order approximation and assumes separate constant flux representations on the edges and interior of the node, that is, $\theta_T = \theta_B = \theta_R = \theta_L = 0$

$$\Psi(x,y) = \psi_{av} \qquad \begin{cases} x_L < x < x_R \\ y_B < y < y_T \end{cases} . \tag{8}$$

The interior source is assumed constant so that $S_x = S_y = 0$ in Eq. (2). Three unknowns remain to be determined, ψ_T, ψ_R, and ψ_{av}. Equation (6) and its x-analog provide two equations with the third equation being the conservation equation found by integrating (1) over the node:

$$\psi_{av} = S_{av}/\sigma - (\psi_R - \psi_L)/\varepsilon_x - (\psi_T - \psi_B)/\varepsilon_y \qquad (9a)$$

ψ_{av} is used to compute the source, S_{av}, for the next iteration. When σ is very small or zero another expression for ψ_{av} can be used. This expression can be obtained using either $\Psi^o(x)$ or $\Psi^o(y)$:

$$\psi_{av} = \int_{y_B}^{y_T} \Psi^o(y)\, dy/\Delta y = \int_{x_L}^{x_R} \Psi^o(x)\, dx/\Delta x \quad .$$

where $\Psi^o(y)$ is given by Equation 6.

CL Scheme

The next higher order nodal scheme is the constant-linear (CL) scheme in which edge fluxes are assumed constant but linear expansions are used for the interior flux. The latter is achieved by adding the terms $\psi_x(2/\Delta x)(x - x_i)$ and $\psi_y(2/\Delta y)(y - y_j)$ to the right side of (8). Equation (2) is used for computing the source. For the five unknowns (ψ_T, ψ_R, ψ_{av}, ψ_x and ψ_y) we use the three equations from the CC method together with fully integrated first moments of (1), namely,

$$\psi_x = S_x/\sigma - (\theta_T - \theta_B)/\varepsilon_y + (6/\varepsilon_x)\left[\psi_{av} - 0.5(\psi_R + \psi_L)\right] \qquad (10a)$$

and

$$\psi_y = S_y/\sigma - (\theta_R - \theta_L)/\varepsilon_x + (6/\varepsilon_y)\left[\psi_{av} - 0.5(\psi_T + \psi_B)\right] \quad . \qquad (10b)$$

Again when σ is very small or zero other expressions for ψ_x and ψ_y can be used. For ψ_y,

$$\psi_y = \int_{y_B}^{y_T} (6/\Delta y^2)(y - y_j)\, \Psi^o(y)\, dy \quad . \qquad (10c)$$

For ψ_x,

$$\psi_x = \int_{x_L}^{x_R} (6/\Delta x^2)(x - x_i)\, \Psi^o(x)\, dx \quad . \tag{10d}$$

For the CL scheme, of course, all ϑ terms in (10) are zero. The moments ψ_x and ψ_y are used to compute S_x and S_y for the next iteration. The five equations in five unknowns are easily reduced by hand for computer coding purposes.

The remaining three schemes use linear expansions both for node edges [see Eq. (3)] and the node interior.

LL1 Scheme

In the LL1 method we approximate the outflow edge first moments by

$$\theta_T = \psi_R - \psi_{av} \tag{11a}$$

$$\theta_R = \psi_T - \psi_{av} \quad . \tag{11b}$$

These equations along with (6) and its x-analog provide four equations for the four outflow edge unknowns ψ_T, θ_T, ψ_R, θ_R. Again this system of four equations in four unknowns is easily solved by hand with the algebra being uncomplicated and operations few. ψ_{av}, ψ_x and ψ_y are determined as in the CL scheme and are used to compute the source for the next iteration.

LL2 Scheme

This scheme is similar to the LL1 scheme. The difference is that the outflow edge moments are approximated by

$$\Theta_T = \psi_x \quad , \tag{12a}$$

$$\Theta_R = \psi_y \quad . \tag{12b}$$

The relations (12) along with equations (10) can be used to determine Θ_T and Θ_R. Since Θ_R does not appear in the equation for Θ_T and vice versa, the system of four equations and four unknowns is easily solved by hand as in the LL1 scheme. Again the algebra is quite simple.

LL3 Scheme

In the LL3 scheme we include a bilinear term ψ_{xy},*(2/Δx)(2/Δy)(x - x_i)* (y - y_j), in the flux expansion over the node interior but retain linear expansions for the source and node edge fluxes. We approximate the outflow edge first moments by

$$\vartheta_T = \psi_x + \psi_{xy} \tag{13a}$$

$$\theta_R = \psi_y + \psi_{xy} \tag{13b}$$

and generate an equation for ψ_{xy} by taking the fully integrated (x - x_i)* (y - y_j) moment of (1). The equations for the remaining unknowns ψ_T, ψ_R, ψ_{av}, ψ_x and ψ_y are the same as for the LL1 and LL2 schemes. However, in contrast to schemes LL1 and LL2, the equations for Θ_T and Θ_R are now coupled to one another. Hence, even though the system of 4 equations in 4 unknowns is still solved by hand before coding, the algebra is much more complicated than in either the LL1 or LL2 schemes.

LL4 Scheme

The final linear-linear scheme, LL4, is a pure nodal scheme. The interior flux is purely linear (not bilinear) and the outflow edge first moments θ_T and θ_R are not approximated. Instead, Eq. (7) and its x-analog are used for determining θ_T and θ_R. As in the LL3 scheme there is coupling between Θ_T and Θ_R as can be seen from Equation (7). The algebra is quite complicated with the number of operations being about the same as for the LL3 scheme.

ADDITIONAL CONSIDERATIONS

Even though negative angular fluxes are a rare occurance for any of these schemes, all can yield negative values for the average outflow fluxes ψ_T and ψ_R. In the higher order methods with a linear internal expansion for the angular flux and a linear expansion for the edge angular flux, Equation (3), negative values can occur for certain x and y. The fix-up used in the code insures that

$$\psi_T + \theta_T * 2(x - x_i)/\Delta x \geq 0 \quad , \tag{14a}$$

$$\text{for } x_{i-\frac{1}{2}} \leq x \leq x_{i+\frac{1}{2}}$$

$$\psi_R + \theta_R \geq 2(y - y_j)/\Delta y \geq 0 \quad , \tag{14b}$$

$$y_{j-\frac{1}{2}} \leq y \leq y_{j+\frac{1}{2}}$$

$$\psi_{av} + \psi_x \geq 2(x - x_i)/\Delta x \geq 0 \quad , \tag{14c}$$

$$x_{i-\frac{1}{2}} \leq x \leq x_{i+\frac{1}{2}}$$

$$\psi_{av} + \psi_y \geq 2(y - y_j)/\Delta y \geq 0 \quad , \tag{14d}$$

$$y_{j-\frac{1}{2}} \leq y \leq y_{j+\frac{1}{2}} \quad .$$

Take (14a) as an example. If $\psi_T < 0$ we set $\psi_T = 0$ and $\theta_T = 0$. If $\psi_T > 0$ but $|\theta_T| > \psi_T$ we set $\theta_T = (\theta_T/|\theta_T|)\ \psi_T$.

In (14c) if $|\psi_x| > \psi_{av}$ we set $\psi_x = (\psi_x/|\psi_x|)\ \psi_{av}$. When the value of either an edge moment (θ) or an interior moment (ψ_x or ψ_y), is recomputed as above, it will be referred to as a "rotation." When a flux (ψ_T or ψ_R) is set to zero, it will be referred to as a fixup.

Care must be taken in solving the equations used in all these schemes as the cross section σ approaches zero. For example quantities such as $[1 - \exp(-\varepsilon_x)]/\varepsilon_x$ appear in the solution equations. The value of this quantity approaches unity as $\sigma \to 0$ and $\varepsilon_x \to 0$. Special programming is required for this and other quantities so that the correct limit is obtained in the computer code. If care is taken the results are found to be well behaved in the limit $\sigma \to 0$.

IV. TEST PROBLEM RESULTS

To test the various nodal method schems, a special version of the TWOTRAN-II[4] production code was created into which all of the various schemes were programmed. Two multigroup test problems were selected for analysis: a ZPPR-7A critical assembly mockup and an iron-water shielding problem. Both problems were analyzed using an S_4 quadrature with isotropic scatter. The Los Alamos CDC-7600 computers were used for the analyses.

ZPPA-7A Problem

Our first test problem was a three-group rectangular geometry ZPPR-7A critical assembly mockup of a heterogeneous fast reactor core as depicted in Fig. 1. In the x-y plane the core configuration is comprised of rectangular "drawers" of about 5.5 cm x 5.8 cm, with 28 drawers in the

x-direction and 29 drawers in the y-direction. Previous analyses of this problem using diamond differencing discrete-ordinates codes[5] showed that the eigenvalue (k_{eff}) for this model was somewhat sensitive to the problem solution mesh used. With one mesh cell per drawer the diamond difference scheme gave a k_{eff} of 0.979 21 while with four (2x2) mesh cells per drawer it yielded a k_{eff} of 0.980 01, a difference of some 0.1%. Accordingly, we used this problem to compare our nodal scheme results to diamond difference results using successive mesh refinements beginning with 1 mesh cell per drawer and ending with sixteen (4x4) mesh cells per drawer. The results are shown in Table 1 along with the computer run times required to achieve the solutions. A convergence criterion of 10^{-4} was used for the eigenvalue, the pointwise fission source, and the pointwise group scalar fluxes. The eigenvalue for an infinitesimally fine spatial mesh is 0.980 28 using our S_4 quatrature.

The CC nodal method scheme described in this paper is not presented in the results. It was found that this scheme was comparable to the diamond scheme in both computer storage and computational efficiency but was less accurate than diamond for eigenvalue problems and, thus, was not considered further.

The CL nodal scheme requires about twice the storage and twice the computational effort as the diamond scheme per mesh point. However, the CL scheme is about twice as accurate as diamond. As seen in Table 1, the CL scheme for a 2x2 mesh per drawer gives about the same accuracy in k_{eff} as does the diamond scheme on a 3x3 mesh per drawer with the computational times roughly equal. Similarly, the CL scheme on a 3x3 mesh per drawer is approximately equivalent to the diamond results from a 4x4 mesh. It thus appears that the CL nodal scheme and the diamond difference scheme are equivalent on an accuracy versus computational cost basis for eigenvalue problems.

The LL1 and LL2 nodal schemes were found to be virtually identical in storage requirements, computational effort, and accuracy. Both require about twice the computer storage and about 2½ to 3 times the computational effort for a given mesh as does the diamond scheme. Table 1 shows, however, that these nodal schemes are about ten times more accurate than diamond. In other words, for a given mesh, the LL1 and LL2 schemes give an eigenvalue whose error is about an order of magnitude less than that obtained with the diamond scheme. Conversely, for a given error in the eigenvalue, the LL1 and LL2 schemes give the same accuracy as diamond on a mesh whose spacing is about three times larger in each direction than that required for diamond. Thus, for the ZPPR-7A problem, the diamond scheme requires a 3x3 mesh per drawer to produce an eigenvalue as good as that from LL1 or LL2 with only 1 mesh cell per drawer; and the computational cost (computer run time) for diamond is about three times as great.

The LL3 and LL4 nodal method schemes were found to be quite similar in their performance and only the LL4 scheme will be considered further. This nodal scheme requires about twice as much storage as the diamond scheme and about four times as much computational effort but it is some 16 times more accurate. Thus, for the ZPPR-7A problem, with 1 mesh cell per drawer, the LL4 nodal schemes gives an eigenvalue as accurate as that obtained using the diamond scheme with 16 (4x4) mesh cells per drawer in about one-fourth the time required by the diamond scheme.

Although only the ZPPR-7A problem results are shown, the nodal method schemes have been compared with the diamond scheme on other eigenvalue test problems with comparable results, namely, for eigenvalue problems nodal method schemes with linear flux expansions both in the mesh cell interior and along the cell edges are about three to four times better than the traditional diamond difference scheme on an accuracy versus computational cost basis.

Iron-Water Shielding Problem

Our second test problem was a three group iron-water shielding problem as depicted in Fig. 2. The central water region contains a spatially uniform, group dependent source. With a group 3 total mean free path of about 1 cm in iron and 0.3 cm in water, the iron shield is 10 mean free paths thick and the outer water shield is over 30 mean free paths thick for group 3. The problem is symmetric in the x- and y-dimensions and uniform square solution meshes were used. Table 2 shows the results of our analyses in which we report the group-dependent net leakages from the system. Exact values for the net leakages were obtained by plotting results and extrapolating to zero mesh size. The "exact" values used are 4.783, 2.515, and 4.811 for group 1 through 3, respectively, with a total source strength of 10^5 particles per second.

In Table 2 we show results only for the CL, LL1 and LL4 nodal schemes. The CC nodal scheme was found to be less accurate than diamond and warranted no further consideration. The LL2 scheme is a virtual twin to the LL1 scheme and the LL3 scheme behaved much like the LL4 scheme.

As a readily evident from Table 2 mesh sizes of about 1 cm (both in x and y) or smaller are required for the diamond scheme to yield realistic results. With a 1 cm mesh spacing the diamond scheme integral quantity results are generally within 10% of the exact, or infinitesimally small mesh, results. To obtain results within 1% of the exact with diamond differencing a mesh spacing of about 0.3 cm or smaller is required.

All of the nodal method schemes give quite similar results for integral quantities, including the CL scheme in which a constant cell (node) edge flux representation is used. The principal differences in the various nodal schemes appear to be the computer run times due to the differences in computational effort. An inspection of pointwise quantities in the detailed results, however, shows a successive improvement in the accuracy of the pointwise quantities produced by the CL, LL1 and LL4 schemes.

Table 2 clearly shows the remarkable superiority of the nodal method schemes over the diamond difference scheme especially for coarse meshing. With a 5 cm mesh spacing the nodal schemes yield excellent leakage values - within 2% of the exact (very fine mesh) values. This accuracy is somewhat misleading, however, and is perhaps anomolously good. Although not shown, we compared average absorption rates within the 5 cm x 5 cm coarse mesh grid shown in Fig. 2. Several of these absorption rates are in error by 10-20% of their exact values. We thus conclude that even with a 5 cm mesh, the nodal schemes give results within 10-20% of the exact results.

With a 2.5 cm mesh spacing the nodal integral quantity results are within 2-4% of the exact results while the diamond scheme yields errors of several hundred percent. Pointwise quantities are somewhat less accurate for all schemes.

When a 1 cm mesh spacing is used the nodal schemes give integral quantity results everywhere within 1% of the exact results. The diamond scheme required a mesh spacing of about 0.3 cm to produce results with comparable accuracy.

The nodal schemes, when applied to deep penetration-type shielding problems are thus capable of producing reliable results with considerally coarser meshes (3 to 5 times coarser in each dimension) than diamond. Although more computationally expensive than the diamond scheme per mesh cell, the greatly reduced number of cells required for the nodal schemes can reduce computer run times by a factor of 3 to 5 when compared with the diamond scheme for the same accuracy.

An interesting and, as yet, not understood result of the shielding problem analysis is the excellent performance of the CL scheme compared with the LL1 and LL4 schemes for producing integral quantities. The CL nodal scheme works just as well as the LL schemes. This is in contrast to the results observed for eigenvalue problems in which the CL scheme was markedly inferior to the linear-linear LL1 and LL4 schemes.

V. SUMMARY AND CONCLUSIONS

A nodal method has been developed for improved spatial differencing of the discrete-ordinates form of the x,y geometry transport equation. In applying this method, spatial flux expansions are assumed along the edges of each solution node (mesh cell) and flux and source expansions are assumed in the interior of the node. Nodal method schemes are thus identified by the expansions used for node edges and node interior. Nodal schemes assuming constant-constant, constant-linear, and four forms of linear-linear expansion have been developed, programmed, and used in the analysis of eigenvalue (k_{eff}) and shielding problems. Nodal results are compared with those obtained using the diamond-difference scheme. Node interior expansions higher than linear have not been considered because of the large increases in computer storage required by higher order expansions.

In the application of these nodal method schemes to the analysis of several problems, two of which are reported in this paper, several important conclusions have been reached.

The constant-constant nodal scheme is less accurate than the traditional diamond-difference scheme and is not considered further.

The constant-linear nodal scheme can be extended to a linear-linear scheme with very little computer storage penalty. The computational effort required by linear-linear schemes is somewhat greater than for the constant-linear scheme.

Based on results from the ZPPR-7A problem and other eigenvalue test problems examined by the authors, it appears that the linear-linear nodal method schemes are more cost effective than the diamond difference scheme for eigenvalue (k_{eff}) problems. These nodal schemes, although more computationally costly than the diamond scheme per mesh cell yield

results of comparable accuracy to those from diamond with far fewer mesh cells. A net savings in both computer time and storage is obtained using the nodal schemes when compared with the diamond scheme for the same accuracy of results.

For shielding problems both the constant-linear and linear-linear nodal schemes are superior to the diamond scheme in the sense of reduced computer time and storage for the same accuracy in results. If only integral quantities such as net leakage or region reaction rates are examined, the constant-linear nodal scheme gives results of comparable accuracy as those from the linear-linear nodal schemes but in less computer time. If, however, local or pointwise quantities are examined, the linear-linear schemes are found to be more accurate than those from the constant-linear scheme. For the same accuracy in local or pointwise quantities, then, the linear-linear schemes are superior.

REFERENCES

1. J. J. Dorning, "Modern Coarse-Mesh Methods - A Development of the '70's," Proc. Amer. Nucl. Soc. Top. Meeting on Computational Methods in Nuclear Engineering Williamsburg, VA, April 23-25, 1979, Vol. 1., pp. 3-1 through 3-31.

2. M. R. Wagner, "A Nodal Discrete-Ordinates Method for the Numerical Solution of the Multidimensional Transport Equation," Proc. Amer. Nucl. Soc. Top. Meeting on Computational Methods in Nuclear Engineering Williamsburg, VA, April 23-25, 1979, Vol. 2, pp. 4-117 to 4-133.

3. R. D. Lawrence and J. J. Dorning, "A Discrete Nodal Integral Transport Theory Method for Multidimensional Reactor Physics and Shielding Calculations," Proc. Amer. Nucl. Soc. Top. Meeting, Sun Valley, Idaho, Sept 14-17, 1980.

4. K. D. Lathrop and F. W. Brinkley, "TWOTRAN-II: An Interfaced, Exportable Version of the TWOTRAN Code for Two-Dimensional Transport," Los Alamos Scientific Laboratory report LA-4848-MS (July 1973).

5. W. F. Miller, Jr., R. E. Alcouffe, G. E. Bosler, F. W. Brinkley, Jr., and R. D. O'Dell, "A Timing Comparison of Two-Dimensional Discrete-Ordinates Codes for Criticality Calculations," Proc. Amer. Nucl. Soc. Top. Meeting on Computational Methods in Nuclear Engineering, Williamsburg, VA, April 23-25, 1979, Vol. 2, pp. 4-1 to 4-18.

Table 1. ZPPR-7A Problem Results

(Convergence Criterion = 10^{-4})

Fine Mesh Points per Drawer	DIAMOND		CL NODAL		LL1 NODAL		LL2 NODAL		LL4 NODAL	
	Run Time, min	k_{eff} (% Error)	Run Time, min.	k_{eff} (% Error)	Run Time, min.	k_{eff} (% Error)	Run Time, min.	k_{eff} (% Error)	Run Time min.	k_{eff} (% Error)
1 x 1	0.7	0.979 21 (-0.109)	0.8	0.980 72 (0.045)	1.0	0.980 12 (-0.016)	1.1	0.980 13 (-0.015)	1.4	0.980 19 (-0.009)
2 x 2	1.5	0.980 01 (-0.028)	2.8	0.980 43 (0.015)	3.6	0.980 26 (-0.002)	4.1	0.980 26 (-0.002)	5.6	0.980 28 (0)
3 x 3	3.3	0.980 16 (-0.012)	6.5	0.980 35 (0.007)	8.6	0.980 27 (-0.001)	8.9	0.980 28 (0)	13.6	0.980 28 (0)
4 x 4	5.7	0.980 21 (-0.007)	11.9	0.980 32 (0.004)	15.7	0.980 28 (0)	16.6	0.980 28 (0)	25.1	0.980 28 (0)

Table 2. Iron-Water Shielding Problem Results

(Convergence Criterion = 10^{-5})

MESH SIZE, cm. (No. of Mesh Points)	DIAMOND				CL NODAL				LLI NODAL				LL4 NODAL			
	Run Time, min.	NET LEAKAGE (% Error)			Run Time, min.	NET LEAKAGE (% Error)			Run Time, min.	NET LEAKAGE (% Error)			Run Time, min.	NET LEAKAGE (% Error)		
		Group 1	Group 2	Group 3		Group 1	Group 2	Group 3		Group 1	Group 2	Group 3		Group 1	Group 2	Group 3
5.0 (10x10 = 100)	0.2	2.337 (-51.1)	3.864 (53.0)	37.39 (677.2)	0.5	4.725 (-1.21)	2.471 (-1.75)	4.805 (-0.12)	0.6	4.748 (-0.73)	2.487 (-1.11)	4.832 (0.44)	0.8	4.742 (-0.86)	2.480 (-1.39)	4.808 (-0.06)
2.5 (20x20 = 400)	0.6	4.115 (-14.0)	2.612 (3.36)	13.60 (182.7)	1.0	4.778 (-0.15)	2.522 (0.45)	4.869 (1.62)	1.6	4.783 (0)	2.527 (0.48)	4.901 (1.87)	2.3	4.781 (-0.04)	2.526 (0.44)	4.899 (1.83)
1.0 (50x50 = 2500)	2.5	4.680 (-2.15)	2.627 (4.45)	5.215 (8.40)	6.8	4.782 (-0.02)	2.519 (0.16)	4.854 (0.89)	9.2	4.783 (0)	2.520 (0.20)	4.857 (0.96)	14.9	4.783 (0)	2.520 (0.20)	4.856 (0.94)
0.5 (100x100 = 10 000)	35.5	4.764 (-0.40)	2.544 (1.15)	4.887 (1.58)	31.7	4.783 (0)	2.517 (0.08)	4.834 (0.48)	63.6	4.783 (0)	2.517 (0.08)	4.835 (0.50)	72.5	4.783 (0)	2.517 (0.08)	4.835 (0.50)
0.333 ... (150x150 = 22 500)	38.9	4.776 (-0.15)	2.526 (0.44)	4.840 (0.60)												

Fig. 1. ZPPR-7A Problem

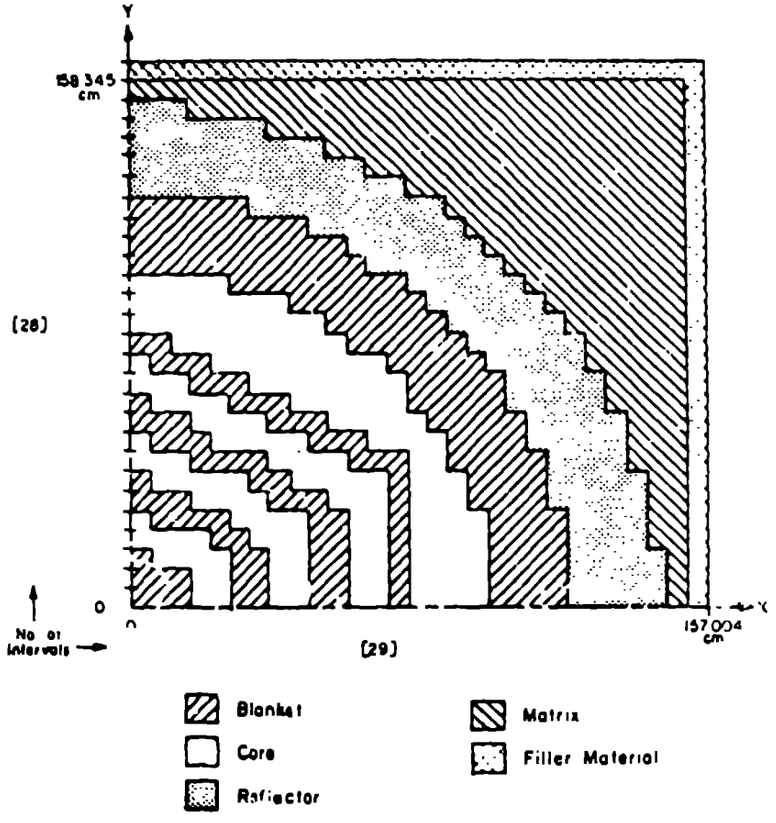

Fig. 2. Iron-Water Shielding Problem